POLITECNICO DI TORINO
Repository ISTITUZIONALE

Enhancing Energy Saving Opportunities through Rightsizing of a Battery Electric Vehicle Powertrain for Optimal Cooperative Driving

Original
Enhancing Energy Saving Opportunities through Rightsizing of a Battery Electric Vehicle Powertrain for Optimal Cooperative Driving / Anselma, Pier Giuseppe; Belingardi, Giovanni. - In: SAE INTERNATIONAL JOURNAL OF CONNECTED AND AUTOMATED VEHICLES. - ISSN 2574-0741. - 3:2(2020), pp. 1-13. [10.4271/12-03-02-0007]

Availability:
This version is available at: 11583/2840433 since: 2020-07-16T10:58:24Z

Publisher:
SAE

Published
DOI:10.4271/12-03-02-0007

Terms of use:

This article is made available under terms and conditions as specified in the corresponding bibliographic description in the repository

Publisher copyright

(Article begins on next page)

19 April 2024

12-03-02-0007

Enhancing Energy Saving Opportunities through Rightsizing of a Battery Electric Vehicle Powertrain for Optimal Cooperative Driving

Pier Giuseppe Anselma, Giovanni Belingardi
Politecnico di Torino, Torino, Italy

Abstract

Current advances in connected and automated mobility claim to change driving scenarios worldwide. Nevertheless, the impact of automated mobility on the design of vehicle powertrains still need exhaustive assessment. In this paper, a design methodology is proposed for BEV powertrains that integrates the consideration of vehicle-to-vehicle (V2V) connected driving. Particularly, each analyzed design solution is evaluated in standard drive cycles both as normal human-operated vehicle and as following car in automated V2V driving. The overall battery energy consumption for the latter case is evaluated by solving an optimization problem to determine off-line the most suitable vehicle speed trajectory. Remaining design requirements include vehicle maximum speed, acceleration capability and gradeability. Obtained results aim at quantifying the amount of energy savings for V2V automated driving depending on the considered mission and BEV powertrain design. Moreover, remarkable changes in the ranking of optimal BEV design solutions are observed based on the specific percentage of the vehicle lifetime travelled as automated following car in the off-line optimized V2V scenario. This work thus represents one of the initial steps to assess the impact of connected and automated driving on the optimal BEV powertrain design solutions.

Keywords

Automated vehicle design; battery electric vehicle; component sizing; connected driving; electric powertrain; energy saving; optimal automated driving; optimal design; vehicle-to-vehicle (V2V)

Introduction

The embedment of advanced driving assistance systems (ADAS) currently represents a common feature of road vehicles [1]. Enhancing comfort and safety particularly constitutes the actual main target for these systems. Related typical examples are cruise control (CC), preserving a desired constant vehicle speed value, and its evolution into adaptive cruise control (ACC), where a safety distance from the preceding vehicle is additionally ensured [2]-[5]. While these systems are already popular and installed on commercially available vehicles, recent research concerning CC aims at implementing novel cooperative adaptive cruise control (CACC) technologies. In CACC, vehicles get information about the longitudinal motion of the preceding vehicle through vehicle-to-vehicle (V2V) wireless communication and automatically adjust their speed accordingly [6][7]. Remarkable system-level benefits can be achieved with these systems including traffic management optimization, fuel economy improvement, emissions reduction, driving comfort enhancement and, above all, safety increase. This latter aspect does not concern vehicle passengers solely, rather it affects the rest of road users as well such as pedestrians, bicyclists and occupants of other vehicles [8]-[10].

V2V communication appears one of the most promising elements to enable automated and connected mobility in the near term. When compared to other intelligences such as vehicle-to-infrastructure communication (V2I), vehicle-to-grid communication (V2G) or vehicle-to-pedestrian communication (V2P), the relative ease of implementation of V2V communication represents a major drive in this framework [11][12]. As example, Toyota and Lexus recently announced the implementation of Dedicated Short-Range Communications (DSRC) systems for V2V interaction on vehicles sold in the United States starting in 2021 [13]. Figure 1 illustrates a sketch of the V2V driving scenario, where the preceding and the following vehicles are named as ‘lead vehicle’ and ‘ego vehicle’ respectively.

Research about V2V interaction range from the perception of the driving comfort [14], through the wireless communication itself [15][16] to the optimal traffic management [17][18]. Moreover, several studies specifically address the reduction of employed vehicular propelling energy through V2V communication between passenger cars. Focusing on internal combustion engine (ICE) vehicles, in 2013 Lang et al. implemented a fuel optimizer control logic for the following vehicle in a V2V scenario and demonstrated that up to 25% fuel economy reduction could be achieved without compromising traffic capacity [19]. The same authors then compared the fuel economy accomplished in an ideal V2V scenario with the corresponding value achievable in CACC without V2V capabilities

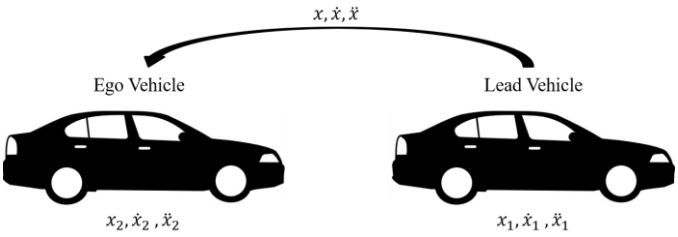

Figure 1. V2V driving scenario.

[20]. In 2017, He and Orosz assessed fuel economy enhancement considering two V2V communication scenarios as well: the first one applied connected cruise control, while the second one implemented model predictive control [21]. As regards hybrid electric vehicles (HEVs), research efforts have demonstrated the capability of improving fuel economy by exploiting information coming from the preceding vehicle in a V2V communication scenario. Analyzed HEV architectures included parallel P0 [22], parallel P2 [23], parallel P1-P4 [24] and power-split [25][26]. Recently, Tate et al. have compared the overall greenhouse gas (GHG) emissions of a traditional ICE vehicle and a battery electric vehicle (BEV) in a V2V scenario. Remarkable reductions could be achieved especially in the BEV case, moreover a down-sizing of the electric motor was declared possible for the following vehicle [27].

Considering two V2V-connected cars, the following vehicle may experience remarkable changes in its automated speed pattern when this latter is optimized according to the information coming from the leading vehicle. Particularly, as a result of the V2V-optimized vehicle operation and usage, smoother drive cycles with a reduced number of stopping events may be experienced by the following vehicle. As consequence, the powertrain may encounter diverse driving requirements according to the vehicle being positioned as leader or follower in a V2V scenario. Changing driving requirements may consequently impact on the optimal design of vehicle powertrains. Despite the aforementioned works aimed specifically at demonstrating the reduction of required propelling energy through V2V communication, little research has been conducted related to optimal powertrain design and sizing while evaluating V2V scenarios. Focusing on BEVs, current powertrain design methodologies only consider a single vehicle travelling in normal driving conditions. A design methodology for BEV powertrains has particularly been proposed based on brute force optimization and traditional driving requirements. Rapid rightsizing of powertrain components was the primary objective of the mentioned research, while up to two gear ratios were found adequate to satisfy the considered BEV driving requirements [28]. This paper aims therefore at developing an optimal design procedure for BEV powertrain that integrates the consideration of V2V automated driving conditions as well. This is achieved by evaluating the BEV electrical energy consumption in an off-line optimized car-following operation for different drive cycles. Obtained results demonstrate that the optimal BEV powertrain sizing may deeply change when considering V2V mobility other than normal driving. The rest of this paper is organized as follows: the retained BEV mathematical model is firstly presented. The subsequent section outlines the optimization problem for determining the energy consumption of a following vehicle in a V2V scenario. The integration of this procedure in a design methodology for BEV powertrains is then discussed. Finally, results and conclusions are given.

Battery Electric Vehicle model

This section aims at detailing the considered mathematical model for BEVs. Figure 2 particularly illustrates a schematic diagram of the model. In this work, an in-body motor powertrain with a single speed transmission (i.e. direct drive) is selected for the analyzed BEVs. Indeed, this layout currently reveals promising being embedded in the majority of commercially available BEVs [29]-[35]. Moreover, our previous work recurrently identified this configuration among the optimal BEV powertrain architectures produced by an automated design methodology [28]. When motoring, the battery delivers electrical energy through the inverter to the electric motor (EM) which in turn propels the vehicle through the transmission system. In a regenerative braking scenario, the energy flow is inverted and the EM functions as a generator. Considering analytical formulations, mathematical models for each retained element of the BEV will be described in the next paragraphs. In general, a backward modelling approach is adopted: taking as input the desired vehicle acceleration or deceleration (a), the model returns as output the corresponding battery State-of-charge (SoC) variation (Δ_{SOC}).

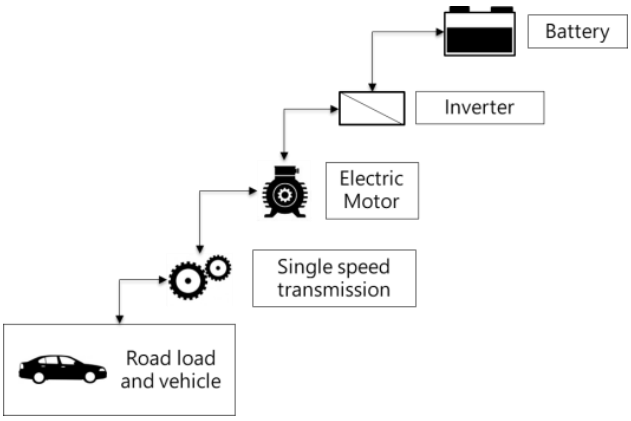

Figure 2. Retained BEV model.

Vehicle and road load

A simple road load approach and a single equivalent mass are considered here to model the vehicle body. More precisely, the transmission output torque T_{OUT} should simultaneously compensate the road resistive loads and satisfy the vehicle acceleration demand (a). This condition can be mathematically expressed in (1).

$$T_{out} = (F_{roll} + F_{misc} + F_{aero} + m_{veh} \cdot a) \cdot r_{wheel}$$

$$\text{With:} \quad F_{roll} = m_{veh} \cdot g \cdot f_0$$

$$F_{misc} = m_{veh} \cdot g \cdot \sin(\alpha) + k \cdot v \tag{1}$$

$$F_{aero} = \frac{1}{2} \cdot \rho \cdot S \cdot C_x \cdot v^2$$

F_{roll}, F_{misc} and F_{aero} are resistive load terms provided by the rolling resistance, some miscellaneous terms (e.g. transmission losses, side forces, road slope) and aerodynamic drag, respectively. m_{veh} and r_{wheel} represent vehicle mass and wheel effective radius, respectively. g, α and ρ stand for the gravity's acceleration, the road slope and the air density, respectively. f_0, k, S and C_x are vehicle parameters corresponding to the rolling friction coefficient, a miscellaneous loss coefficient, the frontal area and the drag coefficient, respectively.

Transmission

Here, the transmission system is considered through (2) and (3) that define the conversion of speed and torque values between input and output of the system (where τ defines the gear ratio).

$$\omega_{EM} = \omega_{out} * \tau \tag{2}$$

$$T_{EM} = \frac{T_{out}}{\eta_{tr}^{sign(T_{out}) * \tau}} \tag{3}$$

ω_{EM} and ω_{out} represent values of angular speed for the EM and wheels, respectively. T_{EM}, the EM torque, can assume positive or negative values depending on propelling or braking conditions. η_{tr} is the efficiency of the transmission system that includes loss of the rotating parts and gear meshing: its value can be assumed constant for preliminary calculations. The sign of the desired transmission output torque as exponent allows accounting for both driving and braking scenarios [36].

Electric motor and inverter

In this paper, the EM is modeled through its empirical loss map that considers core loss, copper loss and mechanical loss of the machine. Starting from this table, it becomes possible to map the EM efficiency according to the corresponding values of speed and torque, as performed in [37][38]. Subsequently, the battery electrical power output (P_{batt}) can be evaluated in (4).

$$P_{batt} = \frac{P_{EM}}{[\eta_{EM}(\omega_{EM},T_{EM})*\eta_{inv}]^{sign(P_{EM})}} + P_{aux} \quad (4)$$

P_{EM} represents the EM output power and demonstrates consistent sign with the EM torque. η_{inv} is the efficiency of the inverter (assumed having a constant value). Retaining the sign of P_{EM} as exponent in the denominator allows capturing both depleting and charging battery conditions within this formula. Finally, P_{aux} is the power requested by the accessories (e.g. lubrication, air conditioning) and is assumed having a constant value here.

Battery

A non-linear Rint model is retained here as a simple equivalent circuit that represents the operation of the battery. The Rint model considers an ideal voltage source (V_{OC}) coupled with a single internal resistance (R_{IN}) that represent the overall behavior of the battery [39]. The efficiency of the battery can thus be calculated in (5).

$$\eta_{batt} = \left(\frac{V_{OC}\cdot I_L - R_{in}\cdot {I_L}^2}{V_{OC}\cdot I_L}\right)^{sign(P_{batt})} \quad (5)$$

I_L represent the battery current and it can be calculated from the value of battery output power. Also in this case both driving and braking scenarios can be considered by introducing an exponential term. Finally, the battery SoC modification between two consequent time steps (Δ_{SOC}) can be evaluated in (6).

$$\Delta_{SOC} = \frac{P_{batt}*\Delta_{time}}{{\eta_{batt}}^{sign(P_{batt})}*C_{batt}} \quad (6)$$

Particularly, Δ_{time} represents the retained simulation time step, whereas C_{batt} stands for the battery capacity.

Optimization problem for V2V driving

In this section, the mathematical problem for determining the optimal operation of the following car in a V2V scenario is presented and discussed. This is performed in order to properly assess the energy economy capability of a specific BEV powertrain design in a car-following automated condition. Particularly, the operation and the driving pattern of the following vehicle is optimized off-line in this case to provide a proper benchmark for the energy usage assessment. In off-line V2V automated driving simulation, the following vehicle ('Ego vehicle') knows a priori beforehand the entire speed profile of the leading vehicle travelling the retained drive cycle. With reference to the V2V scenario reported in Figure 1, at each discretized time instant the Ego vehicle is supposed to receive from the leading vehicle its current values of position, speed and acceleration (x_1, $\dot{x}_1$ and $\ddot{x}_1$respectively). The V2V communication is supposed ideal (i.e. without interaction noise) and instantaneous in this work. Then, the optimal control problem under exam can be formulated in (7).

$$\min\left\{J = \int_{t_0}^{t_{end}} e_{batt}(\dot{x}_2, \ddot{x}_2, t)dt\right\}$$

subject to:

$$\begin{gathered}(x_1 - x_2) \leq d_{MAX} \\ (x_1 - x_2) \geq d_{safety} \\ \ddot{x}_2 \leq \ddot{x}_{2_{max}}(\dot{x}_2)\end{gathered} \quad (7)$$

e_{batt} represents the instantaneous battery energy consumption for the ego vehicle, which is a function of the corresponding vehicle speed ($\dot{x}_2$) and acceleration ($\ddot{x}_2$) values. The distance between lead vehicle and ego vehicle ($x_1 - x_2$), named here inter-vehicular distance (IVD), is then subjected to two constraints. Firstly, its value should not exceed an upper limit (d_{MAX}) in order to both account for physical limitations of the V2V signal transmission and to reduce overall road usage. On the other hand, the IVD should not fall below a critical safety value (d_{safety}) in order to prevent collision. Finally, the vehicle maximum acceleration capability ($\ddot{x}_{2_{max}}$) is considered according to the feasible operating regions of the specific BEV power components. Particularly, a maximum actual value for the vehicle acceleration can be defined as function of the current value of vehicle speed (and, consequently, of EM speed) considering the EM maximum deliverable torque characteristic.

Optimization algorithm

In this paper, dynamic programming (DP) is implemented to solve the introduced optimization problem for V2V automated driving. The DP algorithm examines discretized vectors for the control variable space and the state variable space of the retained mathematical model and returns the global optimal solution by operating an exhaustive search among all the possible control actions at each considered time step. The DP capability of identifying the global optimal solution represents the main reason for its implementation to solve the control problem illustrated in this paper. In 1957, Bellman firstly introduced his principle of optimality laying the foundations for the development of DP [40]. Nevertheless, the widespread usage of DP was made possible only in early 2000s thanks to related advances in the commonly available computational power. DP indeed exhibits remarkable computational costs to perform an exhaustive search through the entire control and state vectors at each considered time step and consequently identify optimal control actions. Its process is implemented backward from the final drive cycle time point to the initial one by searching for the optimal trajectory among the discretized grid points, as illustrated in Figure 3. Particularly, the Bellman's principle of optimality states that the optimal policy can be obtained if a single-stage sub-problem involving only the last stage is solved first, then the sub-problem involving the last two stages, last three stages, etc. until the entire problem is solved step by step. Recently, the DP algorithm has remarkably increased its popularity thanks also to its widespread implementation for effectively solving the optimal control problem for HEV powertrains. Related examples of DP application for HEVs can be found in [41]-[43].

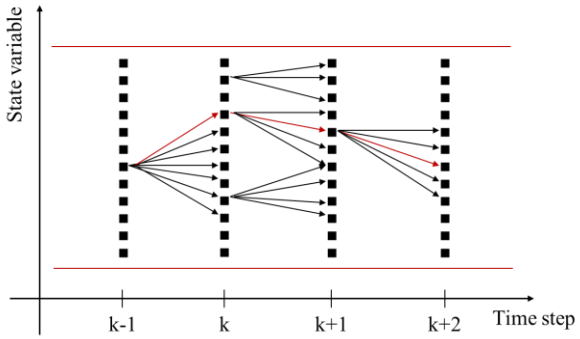

Figure 3. Dynamic programming process.

The adaption of DP algorithm implemented in this paper refers to the version provided by Sundstrom and Guzzella [44]. In order to solve the optimization problem illustrated in (7), considered control variable space (U) and state variable space (X) are reported in (8).

$$U = \{\ddot{x}_2\} \ , \ X = \begin{Bmatrix} x_1 - x_2 \\ \dot{x}_2 \end{Bmatrix} \tag{8}$$

Particularly, U contains the Ego vehicle acceleration value, while X include current values for the IVD and the Ego vehicle speed. In the rest of this section, details will be provided concerning the implementation of the optimization constraints and the objective function for the optimal control problem reported in (7).

Optimization constraints

The optimal automated speed trajectory of the Ego vehicle is subjected to three constraints reported in (7) and related to the maximum allowed IVD (d_{MAX}), the minimum safety IVD (d_{safety}) and the Ego vehicle acceleration.

Maximum allowed IVD

As regards the maximum achievable IVD (d_{MAX}), a value that depends on the road type is assumed here. As a matter of fact, the IVD should be restrained in urban areas to limit overall road utilization and facilitate smooth traffic flow. Limited vehicle speed values achieved in urban areas are particularly helpful in this intent. On the other hand, this restriction may be relaxed for extra-urban and highway scenarios thanks to the increased road surface available. Enhanced safety margins for the actual IVD could also be achieved in this way accounting for the generally higher values of vehicle speed in these types of road. Maximum allowed IVD values of 40 m and 80 m are particularly retained here for urban and extra-urban/highway driving respectively.

Minimum safety IVD

Among the research conducted on mathematical modeling of safety IVD in V2V driving, Chen et al. in 2013 introduced a formulation accounting for both the current Ego vehicle speed and the difference in speed values between the two vehicles [45]. In the same work, a comparison with a traditional braking model and a time-headway model suggested that the introduced formulation could achieved considerable driving safety and simultaneously accomplish traffic efficiency. In general, the model by Chen et al. supposes that, in an emergency, the Lead vehicle would send a warning message to the Ego vehicle. Subsequently, both vehicles would have to stop completely without colliding. The formulation of d_{safety} thus depends on the sign of the difference in vehicle speed value between Lead vehicle and Ego vehicle. Figure 4 illustrates the speed profiles of the two vehicles during an emergency braking for both cases detailed below. The x axis origin particularly relates to the time instant in which the Lead vehicle sends the warning message to the Ego vehicle and starts braking. The distances travelled by the cars are therefore represented by the areas under the corresponding speed trajectories: red and green areas specifically relate to Lead vehicle and Ego vehicle, respectively. When the Lead vehicle initial speed value ($\dot{x}_1^0$) is lower than the Ego vehicle initial speed value ($\dot{x}_2^0$), the following model holds:

$$d_{safety} = s_2 - s_1$$

where

$$\begin{cases} s_1 = \dfrac{(\dot{x}_2^0)^2}{2 \cdot \ddot{x}_{1_{MAX-}}} \\ s_2 = \dot{x}_2^0 \cdot \left(t_1 + t_2 + \dfrac{t_3}{2}\right) + \dfrac{(\dot{x}_2^0)^2}{2 \cdot \ddot{x}_{2_{MAX-}}} \end{cases} \tag{9}$$

s_1 and s_2 are the distance traveled by the Lead vehicle and the Ego vehicle before reaching a complete stop as shown in Figure 4(a), respectively. $\ddot{x}_{1_{MAX-}}$ and $\ddot{x}_{2_{MAX-}}$ are the maximum attainable deceleration values by the Lead vehicle and the Ego vehicle, respectively. Finally, t_1, t_2 and t_3 stand for the system reaction time, the braking coordination time and the required time to reach the complete acceleration capability for the Ego vehicle, respectively.

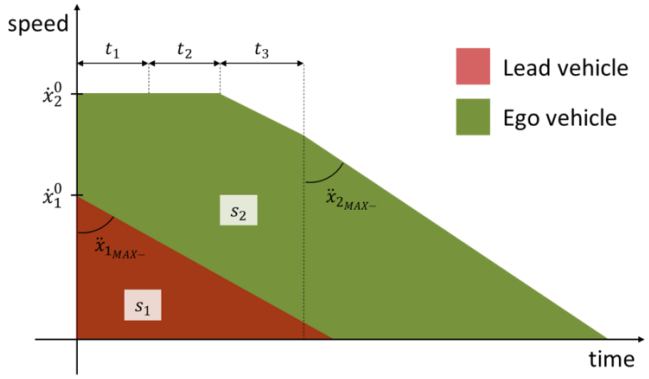

(a) Lead vehicle initial speed < Ego vehicle initial speed

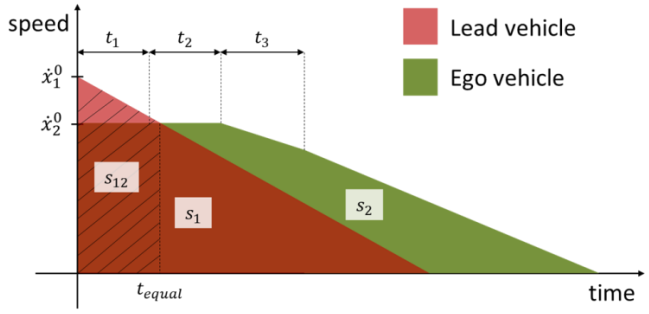

(b) Lead vehicle initial speed > Ego vehicle initial speed

Figure 4. Speed profiles and distances travelled for a V2V emergency braking.

On the other hand, if the Lead vehicle initial speed is greater than the Ego vehicle initial speed, the model for determining d_{safety} in (10) reveals more optimistic in removing the contribution of the distance travelled by both vehicles before exhibiting equal speed values (s_{12}). This latter term can be visualized as the crosshatched area in Figure 4(b).

$$d_{safety} = s_2 - s_1 - s_{12}$$

where

$$\begin{cases} s_{12} = \dfrac{(\dot{x}_1^0)^2 - (\dot{x}_2^0)^2}{2 \cdot \ddot{x}_{1_{MAX-}}} - \dot{x}_2^0 \cdot t_{equal} \\ s_1 = \dfrac{(\dot{x}_2^0)^2}{2 \cdot \ddot{x}_{1_{MAX-}}} \\ s_2 = \dot{x}_2^0 \cdot \left(t_1 + t_2 + \dfrac{t_3}{2}\right) + \dfrac{(\dot{x}_2^0)^2}{2 \cdot \ddot{x}_{2_{MAX-}}} \\ t_{equal} = \dfrac{\dot{x}_1^0 - \dot{x}_2^0}{\ddot{x}_{1_{MAX-}}} \end{cases} \quad (10)$$

s_{12} is the additional term in this case representing the difference between the Lead vehicle displacement and the Ego vehicle displacement during the time period needed for both cars to have the same value of speed (t_{equal}). Apart from this term, the model reveals the same formulation as (9).

Further details for the illustrated safety IVD model can be found in [45]. By applying the reported formulations, it becomes thus possible to map d_{safety} with Ego vehicle speed and relative vehicle speed as independent variables, as illustrated in Figure 5.

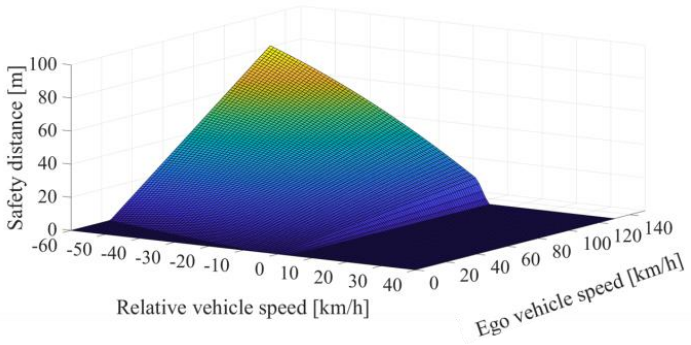

Figure 5. Map of the minimum saftety IVD constraint.

BEV acceleration capability

In solving the optimization problem for V2V driving, a constraint needs implementation to account for the physical limitations in the amount of torque deliverable from the analyzed BEV powertrain. Indeed, the current maximum value of achievable vehicle acceleration is directly proportional to the torque value as stated in (1). According to the typical EM characteristic, the maximum value of deliverable torque gradually decreases when higher angular speed values are reached by the machine. Moreover, physical limitations for the peak power attainable by the battery are retained in (4) in this paper. When the BEV is braking, higher values of decelerating torque can be retained with respect to the limit achievable by the electrical powertrain accounting for the additional contribution of friction braking. Nevertheless, the additional energy term related to friction braking cannot be stored in the battery for future usage, therefore the DP optimization for driving the Ego vehicle in a V2V scenario will likely tend to avoid employing friction braking.

Objective function

When generally implementing DP for vehicle control, defining the objective function to minimize represents a crucial step. In fact, other than the primary optimization target, the objective function usually must include other terms as well to support realistic driving conditions. Here, exclusively minimizing the overall battery energy consumption for the analyzed drive cycle as stated in (7) would particularly lead to "jerky" vehicle speed profiles for the Ego vehicle in the automated V2V scenario [46]. In fact, the DP optimizer would attempt to recover as much regenerative braking energy as possible in this way. Particularly at vehicle speed closed to the null value, an energy-only optimized trajectory would prefer to operate high-frequency fluctuations rather than smooth coasting. A related example of a "jerky" speed profile obtained through a single-term objective function for an Ego vehicle is illustrated in Figure 6 (a). Nevertheless, similar speed profiles would remarkably compromise the travelling comfort for the passengers of the Ego vehicle. A solution to consider the feasibility of driving patterns for the following car in a V2V scenario needs therefore achievement. A first possible option could envisage the addition of a third term in the state variable space (X) in (8) represented by the Ego vehicle acceleration value ($\ddot{x}_2$). Possible constraints to limit the recurrent switch between positive and negative values of vehicle acceleration could thus be implemented in the DP optimization. However, the addition of a further term in the state variable space (X) would increase the

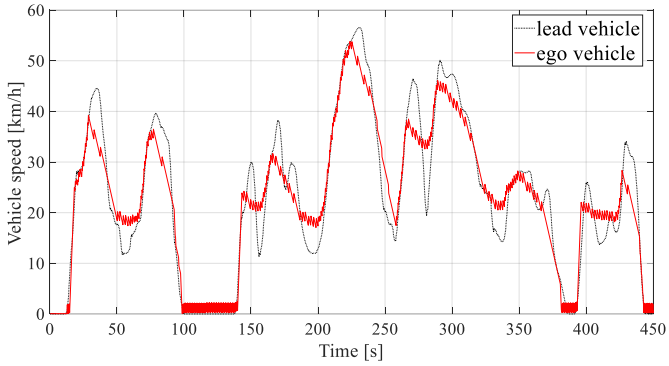

(a) Single-term objective function

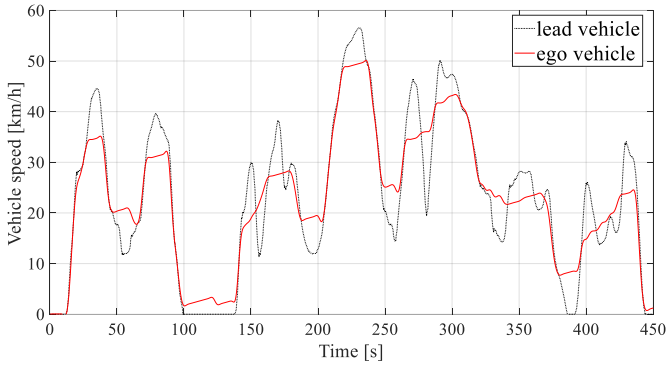

(b) Dual-term objective function

Figure 6. Examples of Ego vehicle speed profile in optimized V2V driving.

dimension of the search space explored by DP. Therefore, an exponential increase in the computational cost for completing the DP optimization procedure may be observed. This could represent a major restriction in implementing a computationally efficient sizing methodology for BEV powertrains, where a large number of design candidates and driving conditions needs to be evaluated. To overcome this draft, in this paper we propose to directly include a penalization term for excessive "jerky" driving in the DP objective function (J_{DP}), as reported in (11).

$$J_{DP} = \int_{t_0}^{t_{end}} [e_{batt}(\dot{x}_2, \ddot{x}_2, t) + \alpha_{jerk}]\, dt \qquad (11)$$

J_{DP} thus include both a first term for the battery energy consumption, and a second term that accounts for jerky driving. α_{jerk} is particularly defined in (12) for this paper.

$$\alpha_{jerk} = \begin{cases} 0 & \ddot{x}_2 \geq 0 \\ \Gamma & \ddot{x}_2 < 0 \end{cases} \qquad (12)$$

Γ represents a coefficient for jerk minimization. Its numerical value should particularly overcome the order of magnitude of the maximum achievable battery power [W] in order to effectively limit the overall percentage of drive cycle spent in braking events. The optimizer will thus keep recovering the highest possible amount of regenerative braking energy, while decelerating the vehicle only when necessary. Figure 6 (b) reports an example for a speed profile of an Ego vehicle when considering the illustrated dual-term J_{DP}. As it can be noticed, smooth and more regular vehicle speed pattern can be achieved in this way for the Ego vehicle with respect to results related to the single-term objective function shown in Figure 6 (a).

BEV design methodology including V2V driving

This section aims at detailing the design methodology for BEV powertrains developed in this paper that aims at integrating the consideration of V2V driving features. The workflow of the entire procedure is illustrated in Figure 7, described as follows and implemented in MATLAB© software.

The design variables for the considered BEV layout include the type and size of EM and the value of the gear ratio for the single speed transmission. A direct search method is applied here in sweeping all the possible combinations of these two design variables. The main reason for not implementing different optimization algorithms to explore the design space (e.g. genetic algorithm, gradient-based optimization, particle swarm optimization) relates in this case to the selected EM being a discrete variable. In fact, each selected EM here represents an actual production component and it is associated with its corresponding operational map as in [28]. Moreover, adopting a direct search approach allows comparing each of the possible design alternatives and assessing their performance singularly.

As common design practice, the following test cases are standardly considered when developing a BEV powertrain [47]:

- Maximum speed
- Acceleration
- Gradeability
- Driving range

Particularly, the first three tests are firstly evaluated as optimization constraints to determine whether the specific BEV powertrain configuration is feasible or not. In Step 3 of Figure 7, the maximum speed achievable by the specific BEV powertrain is firstly assessed. 130 km/h is particularly retained in this paper as the minimum value for the maximum achievable speed by the BEV. Given the large range of operating speed of an EM with respect to an ICE, this constraint is usually satisfied. Considering the production vehicle, it becomes then easy to implement on-board controls to restrict the actual operating map of the EM within the region allowed by the standard maximum speed limits.

As regards acceleration capabilities, a full power 0-100 km/h maneuver is simulated in Step 4 to check whether the analyzed candidate design demonstrates satisfactory performance. The assessed design is particularly kept or discarded depending on the time needed for the maneuver to be completed being lower or greater than a selected time requirement, respectively. The maximum time allowed to complete the maneuver is set to 14 s in this paper. The gradeability potential of successful candidate designs is consequently evaluated in Step 5. The simulation of a vehicle standing start given a certain road slope specifically represents the performance test at this stage. The EM thus must be able to deliver the corresponding requested propelling torque in (13) at null vehicle speed value (T_{EM_start}).

$$T_{EM\_start} \geq \frac{m_{veh} \cdot g \cdot r_{wheel} \cdot (\sin\beta + RL_A)}{\eta_{tr} \cdot \tau} \qquad (13)$$

β represents the slope value that needs to be accomplished, g is the gravity acceleration and RL_A represents the first vehicle road load coefficient (independent on the vehicle speed value). A slope value of 30% is particularly retained in this paper to represent the gradeability requirement.

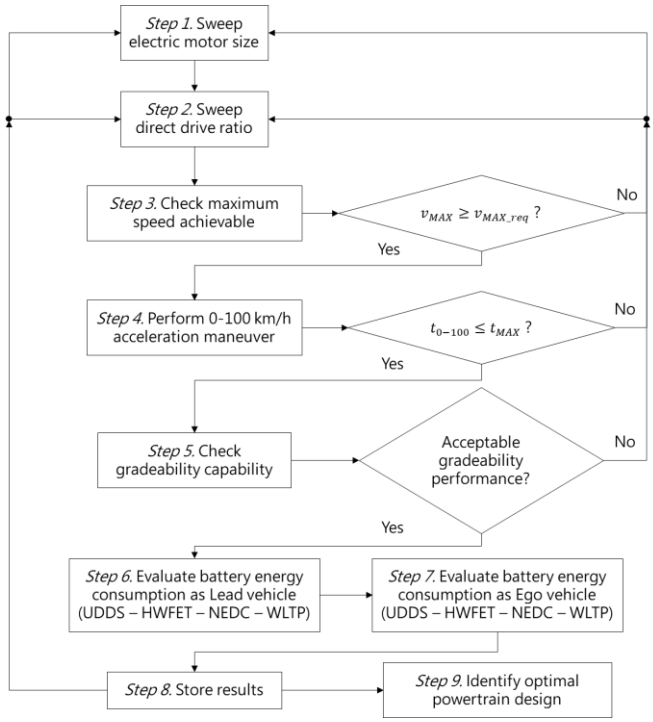

Figure 7. Workflow of the developed BEV powertrain design methodology.

The BEV powertrain designs fulfilling the performance requirements illustrated above are subsequently evaluated in terms of energy consumption (i.e. driving range). The operation of the candidate designs is particularly assessed both in normal driving and as following cars in a V2V scenario in Step 6 and Step 7, respectively. Concerning the normal driving (or Lead vehicle) scenario, the overall energy consumption for each driving mission can be straightforwardly calculated by summing the energy contributions for all the single time points while considering the vehicle model previously introduced. On the other hand, for the car-following case (i.e. Ego vehicle), the optimization problem reported in the previous section requires solving to determine the energy consumption in optimal V2V driving for each assessed candidate design.

Different standard drive cycles are retained here to assess various driving conditions for both the Lead vehicle and the Ego vehicle cases. Considered drive cycles are particularly constituted by the urban driving dynamometer schedule (UDDS), the highway federal test procedure (HWFET), the new European drive cycle (NEDC) and the worldwide harmonized light vehicle test procedure (WLTP). Finally, result for the singularly analyzed driving missions can be averaged to obtain an individual parameter (E_{avg}) that represents the energy consumption of each candidate by adopting the following formulation for both the driving cases:

$$E_{avg} = 0.275 \cdot E_{UDDS} + 0.225 \cdot E_{HWFET} + 0.2 \cdot E_{NEDC} + 0.3 \cdot E_{WLTP} \quad (14)$$

As regards E_{avg}, half of its value can be determined by following the United States Environmental Protection Agency's procedure of retaining 55% weight on the UDDS and 45% on the HWFET. The remaining half of its value can then be evaluated using drive cycles from European Union regulations. In this case, the larger weight for the WLTP can be justified by this procedure aiming at gradually and thoroughly replacing the NEDC.

Following the illustrated design methodology, it becomes possible to identify the optimal BEV powertrain design considering a mixture of Lead vehicle (i.e. human-operated) driving and Ego vehicle (i.e. automated) driving conditions, as it will be detailed in the next section.

Results

This section aims at presenting results obtained by adopting the illustrated methodology and considering a case study BEV. Table 1 particularly reports the vehicle and powertrain data retained in this study. Vehicle data refer to the experimental study conducted in [48], where specific road load coefficients for an actual BEV were determined by removing the drag contribution provided by the EM when coasting. Totally 8 different EMs and 9 transmission ratio values are assessed, thus defining 72 possible powertrain design candidates.

Steps 3 to 6 in the design methodology illustrated in Figure 7 can be generally performed rapidly. On the other hand, solving the optimization problem to assess the energy consumption of the analyzed powertrain design candidate as Ego vehicle in an automated V2V scenario requires considerable computational time. The size for both the discretized control and state vectors amount to 80 elements each in this paper. Then, considering a desktop computer with Intel Core i7-8700 (3.2 GHz) and 32 GB of RAM, Step 7 needs about 16 minutes to be executed for each drive cycle. Therefore, considering the optimization of all the successful design candidates after Step 5 (54 in this paper) for each of the 4 retained drive cycles, overall 16x4x54=3,456 minutes (i.e. about 58 hours) are required to complete the illustrated design methodology.

Table 1. Vehicle and powertrain data.

System	Parameter	Value
Vehicle	Mass [Kg]	1651
	RL_A [N]	116.41
	RL_B [N·s/m]	0.9526
	RL_C [N·s^2/m^2]	0.0399
	r_{wheel} [m]	0.358
Battery	Capacity [Ah]	51
	P_{aux} [kW]	1
EM	Maximum power [kW]	50 ; 60 ; 70 ; 80 ; 90 ; 100 ; 110 ; 120
	η_{inv}	0.95
Transmission	Gear ratio	4.5 : 1 : 12.5
	η_{tr}	0.95
Brake system	t_1[s]	0.2
	t_2 [s]	0.1
	t_3 [s]	0.1
	$\ddot{x}_{MAX}$ [m/s^2]	6.7

Obtained results are divided into two categories in this paper. Firstly, a comparison of energy consumption between Lead vehicle case and Ego vehicle case is presented for three design candidates. The second category of results aims at illustrating how the optimal design solutions vary according to the percentage of vehicle lifetime travelled as automated Ego vehicle in V2V driving.

Quantifying energy saving opportunities in V2V driving

Table 2 specifically reports simulation results for three analyzed BEV powertrain designs both in Lead Vehicle and Ego vehicle cases. Values for the electrical energy consumed by the battery have been normalized according to the distance travelled in each driving mission. In general, by properly solving the optimization problem illustrated above, the energy consumed by the BEV powertrain when travelling as automated Ego vehicle in a V2V scenario diminishes with respect to the normal Lead vehicle case. However, the percentage of energy savings varies according to both the driving conditions and the powertrain parameters. As regards the examined driving mission, higher rates of energy savings can be typically achieved when some distance is covered in an urban environment (e.g. in UDDS, NEDC and WLTP). Lower general values of vehicle speed and frequent stop&start events are particularly favorable in enhancing the amount of energy saved for the Ego vehicle to 10÷20 % in this case.

Table 2. Electrical energy consumption in the analyzed drive cycles.

			Energy consumption [kWh/100 km]											
			UDDS			HWFET			NEDC			WLTP		
Design #	EM size [kW]	τ	Lead Vehicle	Ego vehicle	Δ	Lead Vehicle	Ego vehicle	Δ	Lead Vehicle	Ego vehicle	Δ	Lead Vehicle	Ego vehicle	Δ
1	80	6.5	8.946	8.291	7.9 %	6.838	6.638	3.0 %	8.929	8.310	7.4 %	8.692	7.503	15.8 %
2	90	4.5	9.511	8.264	15.1 %	6.695	6.418	4.3 %	9.092	8.186	11.1 %	8.941	7.372	21.3 %
3	100	4.5	9.498	8.319	14.2 %	6.751	6.472	4.1 %	9.138	8.251	10.8 %	8.952	7.432	20.5 %

An example of simulation results in the WLTP is illustrated in Figure 8 that include time series of the IVD and speed and battery SoC trends for both the Lead vehicle and the Ego vehicle. On the other hand, when exclusively extra-urban and highway driving are included in the considered mission (e.g. HWFET), the amount of energy savings reduces to 3-4 % for the considered parameters. The other variable that may deeply influence the energy savings is represented by the BEV powertrain parameters. As example, in Table 2 the energy consumed in the UDDS by the Design #1 as Lead vehicle is lower than the corresponding value for Design #2. Nevertheless, when considering these designs travelling as Ego vehicles in V2V driving, the ranking according to the energy consumption reverses as the Design #2 overall performs better than Design #1. This suggests that, for the considered example, Design #2 may represent a better solution than Design #1 when the retained BEV travels in optimized V2V automated driving. Therefore, changes in the identified optimal design parameters for the BEV powertrain may be expected when implementing V2V connected driving.

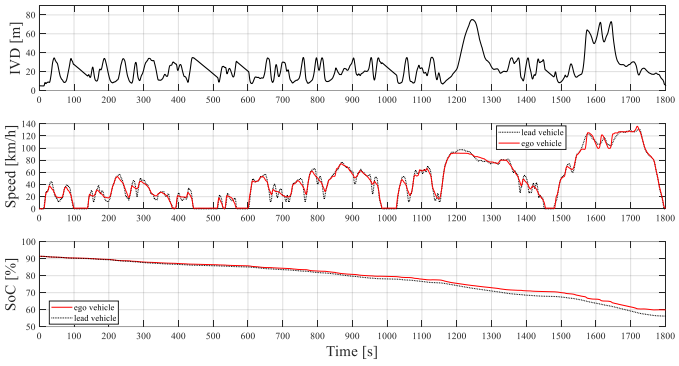

Figure 8. Example of simulation results in the WLTP.

Impacts of V2V driving on the identification of optimal BEV designs

Based on the abovementioned considerations, this paragraph aims at illustrating the impact of connected driving on the ranking of the optimal BEV powertrain designs for the retained vehicle. After completing the illustrated design procedure, different values of E_{avg} for the Lead vehicle case ($E_{avg_{lead}}$) and the Ego vehicle case ($E_{avg_{ego}}$) can be obtained for the successful BEV powertrain designs from (14). Figure 9 particularly illustrates the two Pareto frontiers with 0-100 km/h acceleration time and E_{avg} as independent variables. As highlighted in the plot, the identified optimal design in terms of energy economy differs according whether the vehicle completely travels as Lead vehicle ('Opt. 0% V2V') or as Ego vehicle in V2V driving ('Opt. 100% V2V').

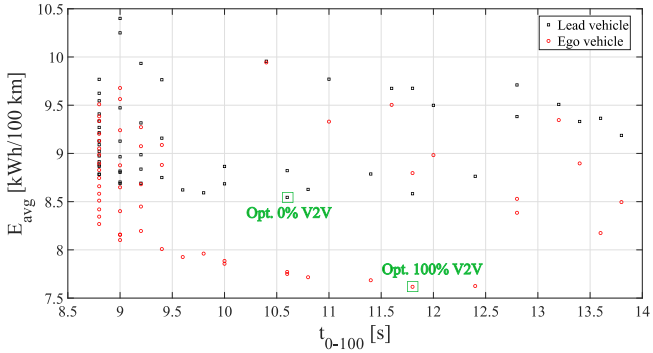

Figure 9. Pareto frontier for Lead vehicle and Ego vehicle cases.

The two Pareto frontiers in Figure 9 respectively represent the actual mobility scenario (where a negligible portion of road vehicles embeds V2V capabilities) and an ideal scenario where the vehicle travels its complete lifetime while getting information from the vehicle ahead (thus similarly to a fully automated mobility scenario). As a matter of fact, new road vehicles in the near future are expected to encounter a mixture of these two extreme driving conditions over their lifetime. Therefore, it becomes necessary to observe how the gradual advancement of connected driving affects correspondingly identified optimal designs. A new parameter, $E_{avg_{mix}}$, thus defines the averaged energy consumption over the total vehicle lifetime as function of the time percentage travelled as Ego vehicle in automated V2V driving ($\%_{V2V}$):

$$E_{avg_{mix}} = \%_{V2V} \cdot E_{avg_{ego}} + (100 - \%_{V2V}) \cdot E_{avg_{lead}} \quad (15)$$

Figure 10 illustrates three new Pareto frontiers obtained when considering the vehicle travelling the 25 %, the 50 % and the 75 % of its lifetime as following car in a V2V scenario, respectively. In general, a gradual decrease in E_{avg} can be observed for all the evaluated designs that is proportional to the level of V2V driving. Moreover, it becomes evident how some BEV powertrain designs demonstrate enhanced capability of reducing their energy consumption through automated V2V driving with respect to other more conservative designs.

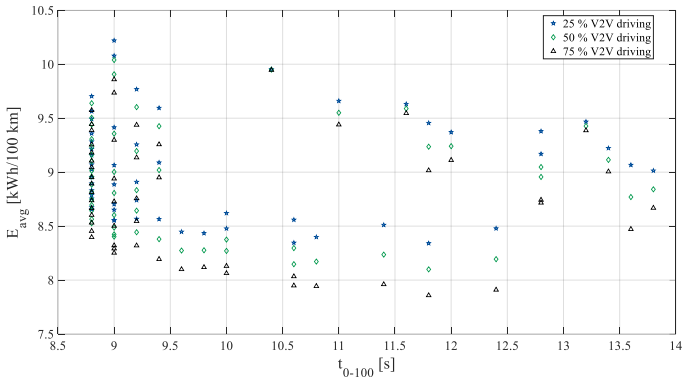

Figure 10. Pareto frontier for mixed normal driving – connected driving cases.

Finally, Table 3 reports the first three optimal designs in terms of energy economy for each retained level of V2V automated driving. The last column of the table confirms how the gradual reduction in the energy consumption is directly proportional to the percentage of V2V driving conducted. For the retained vehicle, the best BEV powertrain design for purely normal driving is thus constituted by the 80 kW EM and the transmission ratio of 6.5. However, as illustrated in Table 2, this design may reveal little improvements when travelling as automated following car in a V2V scenario. In fact, starting from 25 % of V2V driving, the identified optimal transmission ratio modifies into 5.5. Subsequently, when increasing the percentage of automated V2V driving to 75% and 100%, the design with an 80 kW EM and 6.5 transmission ratio is no more included in the three best powertrain designs. On the other hand, different designs related to the EM sizes of 90 kW and 100 kW emerge among the most appealing design solutions. In general, the design candidate with the EM of 80 kW and the transmission ratio of 5.5 appears the most promising solution when considering both normal driving and different percentages of automated V2V driving occurrence.

Table 3. Ranking of optimal designs.

$\%_{V2V}$	Ranking	EM size [kW]	τ	$E_{avg_{mix}}$ [kWh/100 km]
0 %	# 1	80	6.5	10.61
	# 2	80	5.5	11.82
	# 3	80	7.5	9.80
25 %	# 1	80	5.5	8.341
	# 2	80	6.5	8.346
	# 3	90	5.5	8.399
50 %	# 1	80	5.5	8.099
	# 2	80	6.5	8.147
	# 3	90	5.5	8.171
75 %	# 1	80	5.5	7.858
	# 2	90	4.5	7.909
	# 3	90	5.5	7.944
100 %	# 1	80	5.5	7.616
	# 2	90	4.5	7.625
	# 3	100	4.5	7.685

Conclusions

This paper aims at developing an optimal design methodology for BEV powertrains that integrates the evaluation of automated V2V driving. For this reason, an optimization problem to off-line determine the most suitable driving pattern for the following car in a V2V connected scenario is particularly introduced. Solving this problem for each analyzed powertrain design candidate allows estimating the corresponding minimum energy consumption achievable in automated V2V driving conditions. Besides estimating the energy consumption in different standard drive cycles for both normal and automated V2V driving conditions, the implemented design procedure includes the evaluation of the vehicle maximum speed, acceleration capability and gradeability. Here, design variables for the BEV powertrain are represented by the EM type and size and the transmission ratio.

Results obtained from a performed case study firstly demonstrate and quantify the potential reduction of propelling energy required by the automated following car (i.e. Ego vehicle) with respect to the human-operated preceding car (i.e. Lead vehicle) in V2V connected driving. Decreasing the demanded propelling energy may thus result beneficial to address as well the so-called “range anxiety”, which currently represents one of the most contrasting factors to the widespread adoption of BEVs. The amount of reduction in the overall energy needed is found to be affected by both the specific driving conditions and the powertrain design parameters. This suggests that the optimal BEV powertrain design may change when considering a given percentage of the total vehicle lifetime travelled as automated Ego vehicle in V2V driving instead of normal Lead vehicle. Completing the developed design procedure demonstrates how the ranking of the identified optimal design solutions varies according to the percentage of the vehicle lifetime travelled as following car in automated V2V driving. From a general perspective, results obtained in this paper indicate that the increasing spread of connected and automated driving will gradually affect the optimal powertrain design choices for BEVs.

Examples of related future work may consider the implementation of an optimal on-line control strategy to simulate the vehicle travelling as following car in a V2V scenario more realistically. Moreover, more detailed modeling approaches may be adopted for vehicle dynamics and power components (rather than steady-state maps), for the V2V wireless communication and for changes in the aerodynamic drag depending on the IVD. Finally, test cases with more than 2 vehicles may be considered to integrate further connected driving scenarios in the illustrated design methodology.

References

1. Lee, J., Lee, J., Jeong, K., Yoo, S. et al., "Development of a New Neutral Coasting Control Utilizing ADAS and GPS," *SAE Intl. J CAV* 2(2):2019.
2. Winner, H.; Witte, S.; Uhler, W.; Lichtenberg, B. "Adaptive Cruise Control System Aspects and Development Trends", SAE Technical Paper 961010, 1996.
3. Bastian, A., Andreas, P., Holze, R., and Bergholz, R., "Autonomous Cruise Control: A First Step Towards Automated Driving," SAE Technical Paper 981942, 1998.
4. J. Ploeg, B. T. M. Scheepers, E. van Nunen, N. van de Wouw and H. Nijmeijer, "Design and experimental evaluation of cooperative adaptive cruise control," *2011 14th International*

IEEE Conference on Intelligent Transportation Systems (ITSC), Washington, DC, 2011, pp. 260-265.
5. W. Prestl, T. Sauer, J. Steinle, O. Tschernoster, “The BMW Active Cruise Control ACC,” SAE Technical Paper 2000-01-0344, 2000.
6. G. J. L. Naus, R. P. A. Vugts, J. Ploeg, M. J. G. van de Molengraft and M. Steinbuch, "String-Stable CACC Design and Experimental Validation: A Frequency-Domain Approach," in *IEEE Transactions on Vehicular Technology*, vol. 59, no. 9, pp. 4268-4279, Nov. 2010.
7. Tamilarasan, S. and Guvenc, L., "Impact of Different Desired Velocity Profiles and Controller Gains on Convoy Driveability of Cooperative Adaptive Cruise Control Operated Platoons," *SAE Int. J. Passeng. Cars - Mech. Syst.*, 10(1):2017.
8. Hartmann, M., Stolz, M., and Watzenig, D., "Movement Prediction Hypotheses for Pedestrians and Trajectory Planning for Cooperative Driving Systems," *SAE Intl. J CAV* 2(1):17-26, 2019.
9. Joshi, A., "Hardware-in-the-Loop (HIL) Implementation and Validation of SAE Level 2 Automated Vehicle with Subsystem Fault Tolerant Fallback Performance for Takeover Scenarios," *SAE Intl. J CAV* 1(1):13-32, 2018.
10. Gibson, M., Lee, J., Venkatraman, V., Price, M. et al., "Situation Awareness, Scenarios, and Secondary Tasks: Measuring Driver Performance and Safety Margins in Highly Automated Vehicles," *SAE Intl. J CAV* 1(1):33-40, 2018.
11. Chen, Y., Chamadiya, B., and Bueker, U., "V2V Communication - Analysis and Validation of Propagation Models in Real World Scenarios," SAE Technical Paper 2015-01-0289, 2015.
12. Moser, D., Waschl, H., Schmied, R., Efendic, H. et al., "Short Term Prediction of a Vehicle's Velocity Trajectory Using ITS," SAE Int. J. Passeng. Cars – Electron. Electr. Syst. 8(2):2015.
13. IEEE, “Toyota and Lexus to launch DSRC technology to connect vehicles and infrastructure in the U.S. in 2021,” 2018. [Online]. http://sites.ieee.org/connected-vehicles/2018/04/16/toyota-and-lexus-to-launch-dsrc-technology-to-connect-vehicles-and-infrastructure-in-the-u-s-in-2021/, accessed 3 Apr. 2019.
14. Edwards, C., Hankey, J., Kiefer, R., Grimm, D. et al., "Understanding Driver Perceptions of a Vehicle to Vehicle (V2V) Communication System Using a Test Track Demonstration," *SAE Int. J. Passeng. Cars – Mech. Syst.*4(1):444-461, 2011.
15. Wifvat, V., Shaffer, B., and Samuelsen, S., "A Review of Sensor Technologies for Automotive Fuel Economy Benefits," *SAE Intl. J CAV* 2(1):5-16, 2019
16. Bergenhem, C., Coelingh, E., Johansson, R., and Tehrani, A., "V2V Communication Quality: Measurements in a Cooperative Automotive Platooning Application," *SAE Int. J. Passeng. Cars – Electron. Electr. Syst.*7(2):462-470, 2014.
17. Azimi, R., Bhatia, G., Rajkumar, R., and Mudalige, P., "V2V-Intersection Management at Roundabouts," *SAE Int. J. Passeng. Cars - Mech. Syst.*6(2):681-690, 2013.
18. Hallerbach, S., Xia, Y., Eberle, U., and Koester, F., "Simulation-Based Identification of Critical Scenarios for Cooperative and Automated Vehicles," *SAE Intl. J CAV* 1(2):93-106, 2018.
19. Lang, D., Stanger, T., and del Re, L., "Opportunities on Fuel Economy Utilizing V2V Based Drive Systems," SAE Technical Paper 2013-01-0985, 2013.
20. Lang, D., Schmied, R., and Del Re, L., "Prediction of Preceding Driver Behavior for Fuel Efficient Cooperative Adaptive Cruise Control," *SAE Int. J. Engines* 7(1):14-20, 2014.
21. C. R. He and G. Orosz, "Saving fuel using wireless vehicle-to-vehicle communication," *2017 American Control Conference (ACC)*, Seattle, WA, 2017, pp. 4946-4951.
22. Olin, P., Aggoune, K., Tang, L., Confer, K. et al., "Reducing Fuel Consumption by Using Information from Connected and Automated Vehicle Modules to Optimize Propulsion System Control," SAE Technical Paper 2019-01-1213, 2019.
23. F. Zhang, J. Xi and R. Langari, "Real-Time Energy Management Strategy Based on Velocity Forecasts Using V2V and V2I Communications," in *IEEE Transactions on Intelligent Transportation Systems*, vol. 18, no. 2, pp. 416-430, Feb. 2017.
24. Plianos, A., Jokela, T., and Hancock, M., "Predictive Energy Optimization for Connected and Automated HEVs," SAE Technical Paper 2018-01-1179, 2018.
25. Tunnell, J., Asher, Z., Pasricha, S., and Bradley, T., "Toward Improving Vehicle Fuel Economy with ADAS," *SAE Intl. J CAV* 1(2):81-92, 2018.
26. Baker, D., Asher, Z.D., and Bradley, T., “V2V Communication Based Real-World Velocity Predictions for Improved HEV Fuel Economy,” *SAE Technical Paper* 2018-01-1000, 2018.
27. Tate, L., Hochgreb, S., Hall, J., and Bassett, M., “Energy Efficiency of Autonomous Car Powertrain,” SAE Technical Paper 2018-01-1092, 2018.
28. Anselma, P.G., Belingardi, G., “Comparing battery electric vehicle powertrains through rapid component sizing’, *Int. J. Electric and Hybrid Vehicles*, Vol. 11, No. 1, pp.36–58, 2019.
29. Vittone, O. and D'Aprile, F., "New Concepts for the Electrical Fiat Cinquecento," SAE Technical Paper 94A053, 1994.
30. Bitsche, O., "Fully Integrated Electric Vehicle Drive Unit," SAE Technical Paper 951884, 1995.
31. Kamachi, M. and Hosokawa, T., "Study on Practicality of Electric Vehicle “i-MiEV” under Severe Weather," SAE Technical Paper 2011-39-7241, 2011.
32. Shimizu, H., Okubo, T., Hirano, I., Ishikawa, S. et al., "Development of an Integrated Electrified Powertrain for a Newly Developed Electric Vehicle," SAE Technical Paper 2013-01-1759, 2013.
33. Lee, D., Rousseau, A., and Rask, E., "Development and Validation of the Ford Focus Battery Electric Vehicle Model," SAE Technical Paper 2014-01-1809, 2014.
34. Jeong, J., Lee, W., Kim, N., Stutenberg, K. et al., "Control Analysis and Model Validation for BMW i3 Range Extender," SAE Technical Paper 2017-01-1152, 2017.
35. He, S., “NVH Design, Analysis and Optimization of Chevrolet Bolt Battery Electric Vehicle,” SAE Technical Paper 2018-01-0994, 2018.
36. T. Hofman, C. Dai, “Energy efficiency analysis and comparison of transmission technologies for an electric vehicle”, *IEEE Vehicle Power and Propulsion Conference*, Lille, France, 2010, pp. 1-6.
37. A. Mahmoudi, W. L. Soong, G. Pellegrino and E. Armando, "Loss Function Modeling of Efficiency Maps of Electrical Machines," in *IEEE Transactions on Industry Applications*, vol. 53, no. 5, pp. 4221-4231, 2017.
38. Anselma, P. G., Huo, Y., Roeleveld, J., Emadi, A., & Belingardi, G., “Rapid optimal design of a multimode power split hybrid electric vehicle transmission”, *Proceedings of the Institution of Mechanical Engineers, Part D: Journal of Automobile Engineering*, *233*(3), 740–762, 2019.
39. Rolt, R., Douglas, R., Nockemann, P., and Best, R., “Full Battery Pack Modelling: An Electrical Sub-Model Using an EECM for HEV Applications,” SAE Technical Paper 2019-01-1203, 2019.

40. Bellman, R.E., Lee, E., “History and development of dynamic programming”, *Control Systems Magazine, IEEE*, 4(4):24-28, 1984.
41. S. Delprat, J. Lauber, T. M. Guerra, and J. Rimaux,” Control of a parallel hybrid powertrain: Optimal control,” *IEEE Trans. Veh. Technol.*, vol. 53, no. 3, pp. 872–881, May 2004.
42. P.G. Anselma, Y. Huo, J. Roeleveld, G. Belingardi, A. Emadi, “Slope-weighted Energy-based Rapid Control Analysis for Hybrid Electric Vehicles”, *IEEE Transactions on Vehicular Technology*, vol. 68, no. 5, 2019.
43. Debert, M., Colin, G., Chamaillard, Y., Mensler, M. et al., "Energy Management of a High Efficiency Hybrid Electric Automatic Transmission," SAE Technical Paper 2010-01-1311, 2010.
44. O. Sundstrom and L. Guzzella, "A generic dynamic programming Matlab function," *2009 IEEE Control Applications, (CCA) & Intelligent Control, (ISIC)*, St. Petersburg, 2009, pp. 1625-1630.
45. Chen, C., Lü, N., Liu, L. et al., “Critical safe distance design to improve driving safety based on vehicle-to-vehicle communications”, *J. Cent. South Univ.*, 20(11): 3334-3344, 2013.
46. Wuthishuwong, C., Traechtler, A. and Bruns, T., “Safe trajectory planning for autonomous intersection management by using vehicle to infrastructure communication”, *J Wireless Com Network*, 2015: 33, 2015.
47. Sorniotti, A., Subramanyan, S., Turner, A., Cavallino, C. et al., "Selection of the Optimal Gearbox Layout for an Electric Vehicle," *SAE Int. J. Engines*4(1):1267-1280, 2011.
48. Duoba, M. and Jehlik, F., “Investigating Steady-State Road Load Determination Methods for Electrified Vehicles and Coordinated Driving (Platooning),” SAE Technical Paper 2018-01-0649, 2018